

Giant thermal rectification beyond structural asymmetry via current-induced nonreciprocity effects

Jiayao Zhang(张佳瑶), Yu Hao(郝雨), Bowen Xiong(熊博文), Shanhe Su(苏山河), and Zhimin Yang(杨智敏)
Citatio: Chin. Phys. B, 2025, 34 (**9**): 094402. DOI: 10.1088/1674-1056/add906
http://cpb.iphy.ac.cn; http://iopscience.iop.org/cpb

What follows is a list of articles you may be interested in

Influence of substrate effect on near-field radiative modulator based on biaxial hyperbolic materials

Ruiyi Liu(刘睿一), Haotuo Liu(刘皓佗), Yang Hu(胡杨), Zheng Cui(崔峥), and Xiaohu Wu(吴小虎)
Chin. Phys. B, 2024, 33 (**4**): 044403. DOI: 10.1088/1674-1056/ad2a6c

Enhancement of thermal rectification by asymmetry engineering of thermal conductivity and geometric structure for multi-segment thermal rectifier

Fu-Ye Du(杜甫烨), Wang Zhang(张望), Hui-Qiong Wang(王惠琼), and Jin-Cheng Zheng(郑金成)
Chin. Phys. B, 2023, 32 (**6**): 064402. DOI: 10.1088/1674-1056/acc78c

Thermal rectification induced by Wenzel-Cassie wetting state transition on nano-structured solid-liquid interfaces

Haiyang Li(李海洋), Jun Wang(王军), and Guodong Xia(夏国栋)
Chin. Phys. B, 2023, 32 (**5**): 054401. DOI: 10.1088/1674-1056/aca9c1

Contribution of terahertz waves to near-field radiative heat transfer between graphene-based hyperbolic metamaterials

Qi-Mei Zhao(赵启梅), Tong-Biao Wang(王同标), De-Jian Zhang(张德建), Wen-Xing Liu(刘文兴), Tian-Bao Yu(于天宝), Qing-Hua Liao(廖清华), Nian-Hua Liu(刘念华)
Chin. Phys. B, 2018, 27 (**9**): 094401. DOI: 10.1088/1674-1056/27/9/094401

Near-field radiative heat transfer in mesoporous alumina

Li Jing (李静), Feng Yan-Hui (冯妍卉), Zhang Xin-Xin (张欣欣), Huang Cong-Liang (黄丛亮), Wang Ge (王戈)
Chin. Phys. B, 2015, 24 (**1**): 014401. DOI: 10.1088/1674-1056/24/1/014401

SPECIAL TOPIC — Heat conduction and its related interdisciplinary areas

Giant thermal rectification beyond structural asymmetry via current-induced nonreciprocity effects

Jiayao Zhang(张佳瑶)[1], Yu Hao(郝雨)[1], Bowen Xiong(熊博文)[1], Shanhe Su(苏山河)[3], and Zhimin Yang(杨智敏)[1,2,†]

[1] *School of Physics and Electronic Information, Yan'an University, Yan'an* 716000, *China*
[2] *Shaanxi Key Laboratory of Intelligent Processing for Big Energy Data, Yan'an University, Yan'an* 716000, *China*
[3] *Department of Physics, Xiamen University, Xiamen* 361005, *China*

(Received 12 March 2025; revised manuscript received 29 April 2025; accepted manuscript online 15 May 2025)

Pursuing significant thermal rectification effect with minimal temperature differences is critical for thermal rectifiers. While asymmetric structures enable spectral matching, they inherently limit thermal rectification performance. To address this issue, we developed a thermal rectification structure comprising a current-biased graphene-coated silicon carbide (SiC) substrate paired with another graphene-coated SiC substrate separated by a nanoscale vacuum gap. A current-biased graphene sheet generates nonreciprocal effect that actively modulates radiative energy transfer. Our theoretical framework demonstrates that the current-biased graphene achieves a high thermal diode efficiency even under a modest temperature difference. Remarkably, the thermal diode efficiency exceeds 0.8 at a temperature difference of just 100 K (between 300 K and 400 K). These findings highlight the synergistic enhancement from graphene coatings and current biasing, providing a viable strategy for nanoscale thermal management applications.

Keywords: near-field radiative heat transfer, thermal rectification, current-biased graphene, nonreciprocity

PACS: 44.40.+a, 71.36.+c, 78.20.Bh

DOI: 10.1088/1674-1056/add906 **CSTR:** 32038.14.CPB.add906

1. Introduction

Thermal rectification refers to the phenomenon where heat flow in one direction exceeds that in the reverse direction when the hot and cold sources are interchanged. Such devices, termed thermal rectifiers or diodes, hold tremendous potential for thermal management and energy system control. Conventional thermal rectification primarily relied on convection and conduction mechanisms. In contrast, radiative heat transfer, either in the far-field or near-field regimes (subwavelength vacuum gap spacing), is another mode of heat transfer that opens a prominent avenue to explore thermal rectification. Near-field radiative heat transfer (NFRHT) can outperform the blackbody limit through evanescent wave tunneling,[1,2] offering distinct advantages such as high thermal rectification ratios, precise thermal control, and rapid response compared to convection/conduction-based approaches.[3] Furthermore, NFRHT is enhanced if the emitter and receiver materials support surface plasmon polaritons (SPPs), surface phonon polaritons (SPhPs), or hyperbolic modes.[4,5]

Thermal rectification can be achieved through three primary mechanisms: (i) dissimilar materials with temperature-dependent dielectric functions, (ii) asymmetric structures, and (iii) asymmetric interfaces between different materials.[6,7] While dissimilar material pairs induce spectral mismatch that reduces heat flux,[8] asymmetric structures limit the rectification efficiency.[9] Xu *et al.*[10] reported that an indium antimonide (InSb)/graphene-coated silicon carbide (3C-SiC) diode achieved a rectification efficiency over 50% at high and low temperatures of 400 K and 300 K with a 30-nm-wide vacuum gap and a graphene chemical potential of 0.35 eV. Although temperature-dependent dielectrics (e.g., 3C-SiC) enable rectification efficiency, huge temperature differences are required.[6] High temperatures hinder practical applications. Tang and Francoeur reported that a 3C-SiC bulk/3C-SiC thin film diode can sustain a high rectification efficiency ranging from 80% to 87% over a wide high temperature range ($\sim$ 700 K to 1000 K) for a 10-nm-wide vacuum gap.[11] Odebowale *et al.*[3] reported a thermal rectification efficiency of 75% at an emitter temperature of 350 K and a 20-nm-wide vacuum gap by the use of a two-dimensional topological insulator — bismuth selenide (Bi_2Se_3). To break the bottleneck of temperature dependence, the nonreciprocal effect is employed to rectify heat flux.[12,13] The most common way to break reciprocity is by biasing magneto-optical materials with a static magnetic field. Still, this approach is restricted by external bulky biasing circuits and weak nonreciprocal responses at terahertz and optical frequencies.[14] Recent studies demonstrate that applying an electric current to graphene can generate nonreciprocal responses.[15] Graphene, a typical two-dimensional material, supports SPPs that can be controlled from near-

†Corresponding author. E-mail: zhiminyoung@hotmail.com

© 2025 Chinese Physical Society and IOP Publishing Ltd. All rights, including for text and data mining, AI training, and similar technologies, are reserved.

infrared to terahertz frequencies by varying its chemical potential values, which makes it a particularly interesting material in near-field thermal radiation systems.[16] Morgado *et al.*[14] revealed that drift current breaks the reciprocal response of the graphene conductivity and enables a broadband regime of unidirectional SPP propagation. Tang *et al.*[15] studied the near-field heat transfer between graphene and magneto-optic media and found its direction and magnitude can be tuned by the electric current and the in-plane magnetic field in the magneto-optic medium. Peng *et al.*[17] demonstrated a drift-induced radiative heat transfer in double-layer graphene and found a relationship between the heat flux and the current. Ott *et al.*[12] proposed a radiative thermal diode composed of two magneto-optical nanoparticles placed close to a magneto-optical substrate and showed that the rectification coefficient can be actively tuned by changing the magnitude of a magnetic field applied on the system. Yuan *et al.*[13] achieved theoretical rectification ratios over 88.67 through nonreciprocal hyperbolic surface plasmon polaritons, supported by a drift-biased graphene grating, to rectify the radiative heat flux between the two dielectric particles. These advances underscore the potential of nonreciprocal phenomena in developing lower temperature difference thermal diodes. Although sphere-sphere configurations have significant potential to achieve notable thermal rectification efficiency, the limited heat transfer area between particles constrains the overall magnitude of the radiative heat flux. Further exploration of nonreciprocal effects supported by current-biased graphene is important to practical applications of efficient thermal rectifiers under lower temperature differences.

This study investigates how the nonreciprocal effect induced by current-biased graphene influences near-field thermal rectification. We perform comparative analyses of radiative thermal flux for three configurations: bare SiC–SiC, unbiased graphene-coated SiC, and current-biased graphene-coated SiC. Thermal rectification efficiency and the radiative heat flux between two flat surfaces of these configurations at different drift velocities are investigated.

2. Model and theory

The considered structure consists of a high-temperature emitter and a low-temperature receiver separated by a vacuum gap (d), as shown in Fig. 1, where the substrate, graphene, vacuum, graphene, and substrate are denoted by s, 1, 0, 2, and 3, respectively. Bulk SiC is treated as the substrate. The high-temperature emitter is assumed to be made of graphene-covered SiC and maintained at $T_{\mathrm{H}} = 400$ K, and the graphene layer carries a DC electric current induced by a static voltage applied across it. Due to the high mobility of graphene, the electrons in the graphene layer exhibit a drift velocity (v_{d}) of the same order of magnitude as the Fermi velocity (v_{f}).[18] The low-temperature receiver is assumed to be made of graphene-covered SiC and maintained at $T_{\mathrm{L}} = 300$ K.

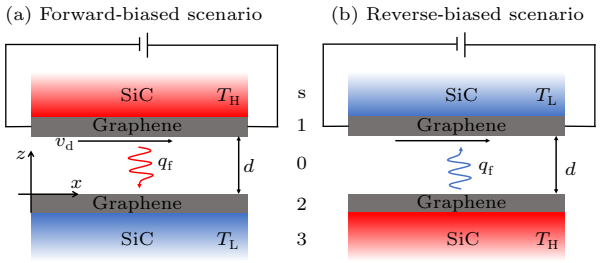


Fig. 1. Schematic image of the near-field thermal rectifier between the graphene-coated plates. (a) Forward-biased scenario and (b) reverse-biased scenario.

In the forward-biased scenario, as shown in Fig. 1(a), the net radiative heat flux between the emitter (current-biased graphene-coated SiC) and the receiver (graphene-coated SiC) is denoted as q_{f}. In the reverse-biased scenario, as shown in Fig. 1(b), the emitter and receiver temperatures are swapped, and the net heat flux is q_{r}. The thermal rectification efficiency, which characterizes the performance of the thermal rectifier, is defined as

$$\varphi = \frac{|q_{\mathrm{f}} - q_{\mathrm{r}}|}{\max(q_{\mathrm{f}},\, q_{\mathrm{r}})}. \tag{1}$$

The net heat flux between two infinite plates separated by a distance d is derived from fluctuation electrodynamics. It is obtained by integrating the spectral heat flux q_ω,

$$q_{\mathrm{f,r}} = \int_0^\infty q_\omega \, \mathrm{d}\omega, \tag{2}$$

where the spectral heat flux is related to the transmission function of both propagating and evanescent waves via Refs. [15, 19].

2.1. Results and discussion

Figure 2 presents the real part of the dielectric function for current-biased and unbiased graphene and SiC. Graphene exhibits strong metallic behavior, characterized by negative $\mathrm{Re}(\varepsilon_{\mathrm{g}})$. Electromagnetic waves can excite surface plasmon polaritons (SPPs), particularly near the plasma frequency. Surface polarization with p polarization can be coupled only when the permittivities of media 1 and 2 have opposite signs.[28] As shown in Fig. 2(a), $\left|\mathrm{Re}(\varepsilon_{\mathrm{g}})\right|$ increases with higher μ_{g}, indicating enhanced metallic behavior dominated by graphene plasmons.[16] Notably, at low frequencies, $\mathrm{Re}(\varepsilon_{\mathrm{g}})$ becomes positive due to the negative $\sigma_{\mathrm{g}}^{\mathrm{e}}$, which induces optical gain and negative Landau damping.[15,29] The excitation of SPPs interacts with incident radiation, leading to strong absorption. In Fig. 2(b), the negative values of $\mathrm{Re}(\varepsilon_{\mathrm{SiC}})$ for SiC appear within the frequency range of 1.5×10^{14} rad/s to 1.8×10^{14} rad/s, giving rise to SPhPs.

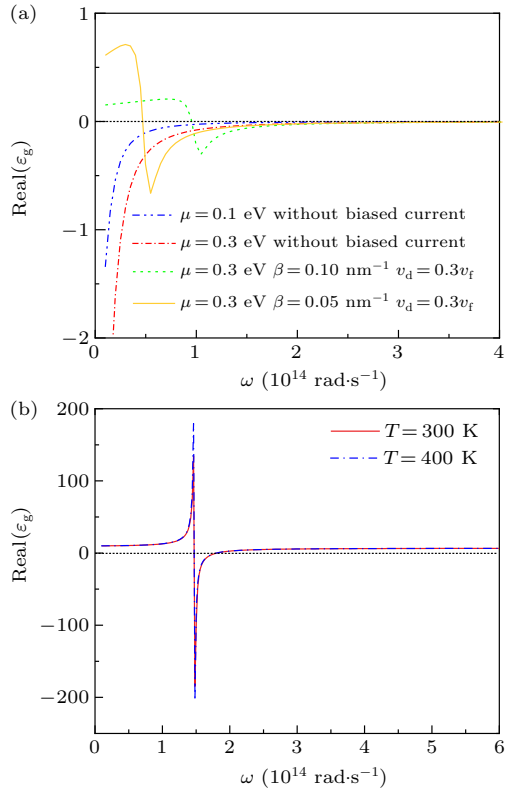


Fig. 2. Real part of dielectric function of (a) graphene at 300 K and (b) SiC.

Figure 3(a) depicts the forward spectral heat flux as a function of angular frequency (ω) for three configurations: bare SiC–SiC bulk, current-biased graphene-SiC bulk, and graphene-SiC bulk, where parameters $d = 10$ nm, $v_d = 0.6v_f$, $\mu_g = 0.4$ eV, and $\gamma_g = 3.7$ meV are maintained unless otherwise stated. In the bare SiC–SiC scenario, a narrow peak with significant monochromaticity emerges at $\omega = 1.76 \times 10^{14}$ rad/s. This arises from thermally excited SPhPs supported by SiC in the frequency range of negative values of $\mathrm{Re}(\varepsilon_{SiC})$ for SiC. Although the thermal diode effect in SiC can be implemented by the temperature dependence of its dielectric function, Fig. 2(b) reveals that this dependence is weak. Consequently, a sizable temperature difference is required to achieve a pronounced thermal diode effect for SiC. For the graphene-coated SiC configurations in Fig. 3(a), two broad peaks are observed. The spectral heat flux of the current-biased graphene-coated SiC configuration is slightly higher than that of the unbiased graphene SiC configuration in most low-frequency regions, with a notable increase in high-frequency regions. This enhancement stems from the photon occupation difference induced by the current-biased graphene, which generates a finite photonic chemical potential. The occupation number of radiative photons becomes nonreciprocal, which can be controlled by the drift velocity of the electric current. To this end, the current-biased configuration achieves the highest heat flux, reaching 1.903×10^6 W/m^2, compared to 1.734×10^6 W/m^2 for unbiased graphene SiC and 0.5620×10^6 W/m^2 for the bare SiC–SiC. To characterize the thermal diode effect caused by the current-biased graphene, Fig. 3(b) plots the forward and reverse spectral heat fluxes at $d = 10$ nm and $v_d = 0.6v_f$. Although the maximum spectral heat fluxes of the unbiased graphene-coated SiC and bare SiC configurations are higher than those of the current-biased graphene-coated SiC configuration, these regions are extremely narrow. Figure 3(b) shows that the forward spectral heat flux is significantly higher than the reverse spectral heat flux, such that the forward thermal flux reaches 1.903×10^6 W/m^2, which is 5.62 times larger than the reverse thermal flux of 0.3386×10^6 W/m^2. The thermal rectifier factor is as high as 0.822 even at a small temperature difference of 100 K. Figure 3 indicates that the proposed structure enables significant thermal rectification under small temperature differences, highlighting its potential for low-energy thermal management applications.

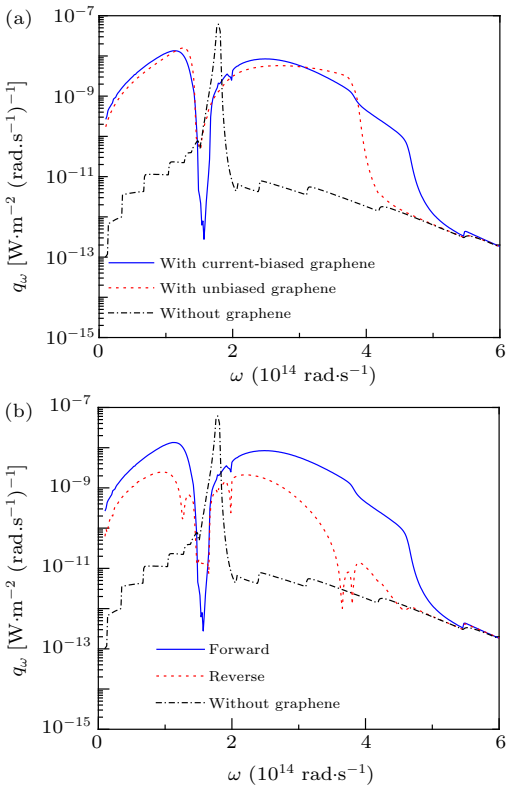


Fig. 3. (a) Forward spectral thermal flux versus angular frequency. (b) Forward and reverse spectral thermal fluxes versus angular frequency at $d = 10$ nm, $v_d = 0.6v_f$, $\mu_g = 0.4$ eV, and $\gamma_g = 3.7$ meV.

Figure 4 illustrates the spectral thermal fluxes in both (a) forward and (b) reverse cases as functions of angular frequency for different v_d at $d = 10$ nm. Two distinct peaks can be observed in Fig. 4. In the forward case (Fig. 4(a)), the narrow peak diminishes while the broader peak rises as v_d increases, leading to an enhancement in the forward thermal flux. This behavior stems from the modulation of the drift velocity on the photon distribution within the graphene layer: higher v_d enhances non-equilibrium photon populations, thereby boosting energy transfer. Conversely, Fig. 4(b)

shows that two peaks of the reverse spectral heat flux increase as v_d decreases. This trend is attributed to the increase in reverse heat flux generated from the current-biased graphene-coated SiC. The photon number $(N_i(\omega, T_i, \beta_x) = [\exp(\hbar(\omega - \beta_x v_d)/(k_B T_i)) - 1]^{-1})$ on the graphene layer increases as v_d increases, allowing more heat flux to propagate from the biased graphene-SiC to the unbiased counterpart.

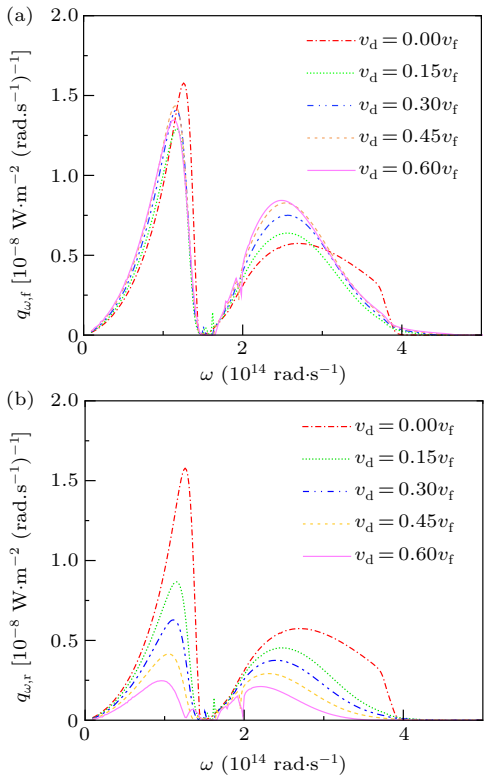


Fig. 4. (a) Forward and (b) reverse spectral thermal fluxes versus angular frequency for different v_d at d =10 nm and μ_g =0.4 eV.

Figure 5(a) displays the ratios of the forward and reverse heat fluxes to the blackbody limit versus gap distance d. Both forward and reverse radiative heat fluxes substantially exceed the blackbody limit. This confirms that narrow gap distance and large temperature differences amplify radiative heat flux. For the same d and v_d, the forward heat flux exceeds the reverse flux, with the difference decreasing as d increases. As shown in Fig. 5(b), the thermal rectification efficiency φ decreases with increasing d because the heat flux differences between the forward and reverse decrease as d increases (see Fig. 5(a)). For instance, at $v_d = 0.6v_f$, φ drops from 0.822 to 0.383 as d increases from 10 nm to 100 nm; at $v_d = 0.3v_f$, φ decreases from 0.526 to 0.214 when d is increased from 10 nm to 100 nm. Note that φ of the bare SiC–SiC configuration equals zero because the forward and reverse heat fluxes of bare SiC–SiC are the same, as shown in Figs. 3(a) and 3(b). Thermal rectification efficiency φ at v_d =$0.6v_f$ is observed to be higher than that at $v_d = 0.3v_f$ when the vacuum gap distances are equal. For $d = 10$ nm, $\varphi = 0.822$ at $v_d = 0.6v_f$ while $\varphi = 0.526$ at $v_d = 0.3v_f$. For $d = 100$ nm, $\varphi = 0.383$ at $v_d = 0.6v_f$ while $\varphi = 0.214$ at $v_d = 0.3v_f$. Figure 5 demonstrates that smaller gap distances and higher drift velocities yield larger thermal diode factors, highlighting the critical role of near-field coupling and nonreciprocal photon transport in enhancing thermal rectification performance.

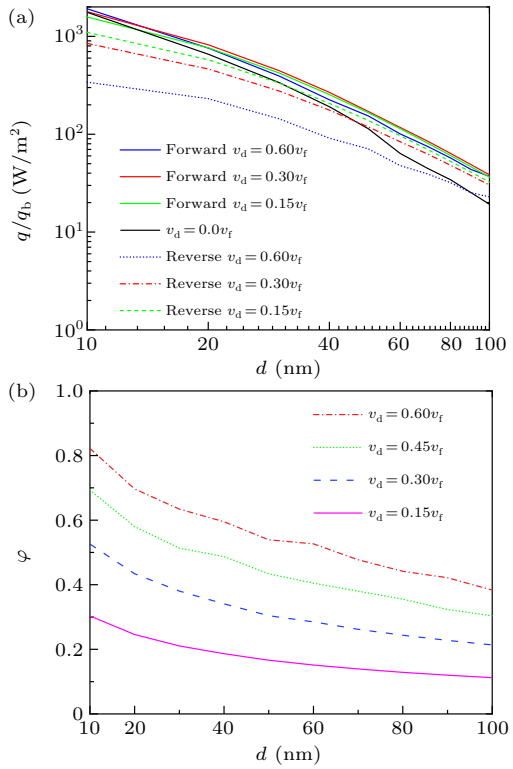


Fig. 5. (a) Ratio of radiative heat flux and (b) thermal rectification efficiency as functions of the gap distance with different v_d at $\mu_g = 0.4$ eV and $\gamma_g = 3.7$ meV.

3. Conclusions and outlook

We proposed a model of a thermal diode comprising two graphene-coated SiC substrates, where a drift current traverses the graphene layer at one terminal. The drift current in the graphene sheet induces a nonreciprocal effect. The impacts of near-field coupling and nonreciprocity on thermal rectification are investigated. Our analysis reveals that, unlike the bare SiC configuration, both unbiased and current-biased graphene-coated SiC configurations exhibit two spectral peaks. Furthermore, the heat flux in these graphene-enhanced configurations surpasses that in the bare SiC configuration. Under drift current conditions, the forward spectral thermal flux is significantly higher than the reverse flux. Specifically, the forward thermal flux attains a peak value of 1.903×10^6 W/m^2 (5.62 times greater than the reverse thermal flux of 0.3386×10^6 W/m^2) at $d = 10$ nm and $v_d = 0.6v_f$. These results highlight the critical role of near-field coupling and nonreciprocal photon transport in enhancing thermal rectification performance. The thermal rectification efficiencies are 0.822 and 0.526 for $v_d = 0.6v_f$ and $v_d = 0.3v_f$ at $d = 10$ nm, respectively.

The proposed thermal rectification structure is theoretically modeled as infinitely large plates. However, actual devices typically have finite dimensions on the microscale or nanoscale. In such cases, the view factor (also known as the shape factor) — a purely geometrical parameter describing the orientation-dependent radiation between surfaces — must be considered. It quantifies the fraction of radiation emitted from one surface that reaches another, ranging from 0 (no direct radiation) to 1 (perfect alignment, as in infinitely large plates). Radiation heat transfer between surfaces depends on their relative orientation, geometric configuration, radiative properties, and temperatures. The view factor, as a key geometric parameter, has a significant effect on the radiative heat loss between the emitter and receiver: a higher view factor reduces such loss by enhancing direct energy transfer, whereas a lower value increases loss due to reduced geometric coupling.[30,31]

Theoretically, a notable thermal rectification efficiency is attainable at a 10 nm vacuum gap. While experiments of NFRHT have been conducted with tip–plane, sphere–plane, and plane–plane configurations, plane–plane configurations are preferable for energy-related applications of thermal radiation (e.g., thermophotovoltaic devices, radiative cooling, and active heat control) due to their large heat transfer area. Although plane–plane NFRHT has been verified down to gap distances as small as ~ 7 nm,[32] maintaining a precise parallel nano-gap between macroscale plates remains a significant experimental challenge.[33,34] Nonetheless, thermal rectification in near-field thermal radiation at elevated temperatures has been experimentally demonstrated, achieving a maximum rectification efficiency of 10.9% at terminal temperatures of 375 K and 530 K with an initial separation gap of 3 μm.[35] More recently, graphene-enabled enhancement of near-field radiative heat flux between two planar dissimilar dielectric media has been experimentally verified for vacuum gaps in the range of 100–140 nm.[36] These prior studies provide a solid foundation for further experimental validation of the nonreciprocal near-field thermal diode.

This study highlights that nonreciprocal effects in plane–plane configurations can significantly boost the thermal rectification efficiency, beyond traditional approaches like temperature-dependent materials. In addition to current-biased graphene, Weyl semimetals have emerged as promising candidates, offering nonreciprocal thermal responses without requiring an external magnetic field — a critical advantage over graphene-based systems that often rely on current biasing.[37,38] Beyond Weyl semimetals, topological materials, such as Dirac semimetals, also exhibit remarkable capabilities to enhance or suppress near-field thermal radiation. Dirac semimetals can actively modulate the heat flux by tuning geometric parameters, the Fermi level, and the degeneracy of three-dimensional (3D) Dirac points.[39] Such materials open new avenues for efficient thermal rectification at moderate gaps and low temperature differences.

Acknowledgments

Project supported by the National Natural Science Foundation of China (Grant No. 12364008), the Ph. D. Research Startup Foundation of Yan'an University (Grant No. YDBK2019-54), and the Yan'an High-level Talent Special Project (Grant No. 2019263166).

References

[1] Basu S, Zhang Z M and Fu C J 2009 *Int. J. Energ. Res.* **33** 1203
[2] DeSutter J, Tang L and Francoeur M 2019 *Nat. Nanotechnol.* **14** 751
[3] Odebowale A A, As'ham K, Berhe A M, Alim N, Hattori H T and Miroshnichenko A E 2024 *Int. Commun. Heat Mass Transfer.* **157** 107707
[4] Tian P, Ge W, Li S, Gao L, Jiang J and Xu Y 2023 *Chin. Phys. Lett.* **40** 067802
[5] Han X Z, Zhang J H, Liu H T, Wu X H and Leng H W 2024 *Chin. Phys. B* **33** 047801
[6] Wang L P and Zhang Z M 2013 *Nanosc. Microsc. Therm.* **17** 337
[7] Du F Y, Zhang W, Wang H Q and Zheng J C 2023 *Chin. Phys. B* **32** 064402
[8] Zhang W B, Wang B X and Zhao C Y 2022 *Int. J. Heat Mass Transfer.* **188** 122588
[9] Xu G, Sun J, Mao H and Pan T 2018 *J. Quant. Spectrosc. RA* **220** 140
[10] Xu G, Sun J, Mao H and Pan T 2018 *J. Appl. Phys.* **124** 183104
[11] Tang L and Francoeur M 2017 *Opt. Express* **25** A1043
[12] Ott A, Messina R, Ben-Abdallah P and Biehs S A 2019 *Appl. Phys. Lett.* **114** 163105
[13] Yuan M Q, Zhang Y, Yang S H, Zhou C L and Yi H L 2022 *Int. J. Heat Mass Transfer.* **185** 122437
[14] Morgado T A and Silveirinha Mário G 2022 *Nanophotonics* **11** 4929
[15] Tang G, Zhang L, Zhang Y, Chen J and Chan C T 2021 *Phys. Rev. Lett.* **127** 247401
[16] Chang J Y, Yang Y and Wang L 2016 *J. Quant. Spectrosc. Radiat. Transfer.* **184** 58
[17] Peng J and Wang J S 2018 arXiv:1805.09493 [cond-mat.mes-hall]
[18] Morgado T A and Silveirinha M G 2017 *Phys. Rev. Lett.* **119** 133901
[19] Kan Y H, Zhao C Y and Zhang Z M 2020 *Phys. Rev. Appl.* **13** 014069
[20] Francoeur M, Meng M P and Vaillon R 2010 *J. Phys. D: Appl. Phys.* **43** 075501
[21] Messina R, Antezza M and Ben-Abdallah P 2012 *Phys. Rev. Lett.* **109** 244302
[22] Xu G, Sun J, Mao H and Pan T 2020 *Int. J. Therm. Sci.* **149** 106179
[23] Zhu L, Otey C R and Fan S 2013 *Phys. Rev. B* **88** 184301
[24] Habibzadeh M, Islam M S and Edalatpour S 2023 *J. Quant. Spectrosc. RA* **307** 108662
[25] Feng D, Yang X, Han Z and Ruan X 2024 *Phys. Rev. B* **109** L081409
[26] Baltaji R and Kazan M 2019 *J. Appl. Phys.* **125** 065102
[27] Lim M, Lee S S and Lee B J 2013 *Opt. Express* **21** 22173
[28] Park K and Zhang Z M 2013 *Front. Heat Mass Trans.* **4** 1
[29] Liu R Y, Liu H T, Hu Y, Cui Z and Wu X H 2024 *Chin. Phys. B* **33** 044403
[30] Nassar Y F 2020 *Int. J. Heat. Mass. Tran.* **159** 120130
[31] Chen M, Yan H, Zhou P and Chen X Y 2020 *J. Quant. Spectrosc. RA* **253** 107163
[32] Salihoglu H, Nam W, Traverso L, Segovia M, Venuthurumilli P K, Liu W, Wei Y, Li W and Xu X 2020 *Nano Lett.* **20** 6091
[33] Ghashami M, Jarzembski A, Lim M, Lee B J and Park K 2020 *Annu. Rev. Heat Trans.* **23** 13
[34] Zhang J, Shi K, Lu L, Feng D, Liu H and Wu X 2023 *Clean Energy Sci. Technol.* **1** 45
[35] Elzouka M and Ndao S 2017 *Sci. Rep.* **7** 44901
[36] Habibzadeh M, Islam M S, Chow P K and Edalatpour S 2024 *Acs Photonics* **11** 4101
[37] Guo C, Zhao B, Huang D and Fan S 2020 *Acs Photonics* **7** 3257
[38] Wu J, Li H, Fu C and Wu X 2023 *Int. J. Therm. Sci.* **184** 107902
[39] Didari-Bader A, Kim S, Choi H, Seo S, Biswas P, Jeong H and Lee C W 2024 *Mat. Today Phys.* **46** 101489